Optimal Scheduling of Distributed Energy Resources and Responsive Loads in Islanded Microgrids Considering Voltage and Frequency Security Constraints

Vahedipour-Dahraie, Mostafa; Najafi, Hamid Reza; Anvari-Moghaddam, Amjad; Guerrero, Josep M.

Published in:
Journal of Renewable and Sustainable Energy

DOI (link to publication from Publisher):
10.1063/1.5027416

Publication date:
2018

Document Version
Accepted author manuscript, peer reviewed version

Optimal Scheduling of Distributed Energy Resources and Responsive Loads in Islanded Microgrids Considering Voltage and Frequency Security Constraints

Mostafa Vahedipour-Dahraie[1], Hamid Reza Najafi[1,*], Amjad Anvari-Moghaddam[2], Josep M. Guerrero[2]

[1] Department of Electrical & Computer Engineering, University of Birjand, Birjand, Iran; vahedipour_m@birjand.ac.ir

[2] Department of Energy Technology, Aalborg University, Aalborg, Denmark; aam@et.aau.dk; joz@et.aau.dk

***Corresponding Author:** Hamid Reza Najafi, h.r.najafi@birjand.ac.ir; **Tel:** +98 (56)32202049

Abstract

Low inertia of distributed energy resources (DERs), high penetration levels of renewable energy sources (RESs) and load demand variations put the islanded microgrids (MGs) security at risk of instability. This paper proposes a two-stage stochastic model for coordination of DERs and responsive loads in islanded MGs with regard to voltage and frequency security constraints. Based on the proposed model, scheduling of the controllable units in both supply and demand sides is done in a way not only to maximize the expected profit of MG operator (MGO), but also to minimize the energy payments of customers under the premise of security and stability of MG. An AC optimal power flow (AC-OPF) procedure is also used to study operating condition of the system under uncertainties and to guarantee acceptable nodal voltages and system frequency during different scenarios. The proposed stochastic optimization model is then applied to a typical autonomous MG and its effectiveness is demonstrated through different scenarios under uncertainties in load consumption and renewable energy resources (RESs) productions. Simulation results demonstrate that customers' participation in DR programs have significant effect on the system's performance in terms of voltage and frequency stability. Moreover, optimal coordination of DERs and responsive loads can increase the expected profit of MGO significantly. The effectiveness of the proposed scheduling approach is verified on an islanded MG test system over a 24-h period.

Index Terms—Demand response (DR), microgrid (MG), distributed energy resource (DER), voltage and frequency security, renewable energy sources (RESs).

Nomenclature

N_G , N_W , N_V	Number of DG, wind and PV units.
N_J , N_S , N_T	Number of load groups, scenarios and time periods.
i , w , v	Indices of DG, wind and PV units.
j , s , t	Indices of load groups, scenarios and time periods.
b, n, r	Indices of system buses.
$B(D_{j,t}^{DR})$	Income of group *j* of customer at period t after implementing DR programs.
$B_{j,t}^{0}$	Income of group *j* of customer at period *t* when the demand is at nominal value.
$C_{w,t}$ ($C_{v,t}$)	Energy bid submitted by wind unit *w* (PV *v*) in period *t* (cents/kWh).
$C_{i,t}^{R^U}$ ($C_{i,t}^{R^D}$)	Bid of the up (down)-spinning reserve submitted by DG i in period *t* (cents/kWh).
$C_{i,t}^{R^{NS}}$	Bid of the non-spinning reserve submitted by DG *i* in period *t* (cents/kWh).
$C_{j,t}^{R^U}$ ($C_{j,t}^{R^D}$)	Bid of the up (down)-spinning reserve submitted by load *j* in period *t* (cents/kWh).
$D_{j,t}$ ($D_{j,t,s}$)	Demand of load *j* in period *t* (and scenario *s*) (kW).
$D_{j,t}^{DR}$	Demand of load group *j* after implementing DR programs in period *t* (kW).
$E_{j,t,t}$ ($E_{j,t,h}$)	Self-elasticity (Cross-elasticity) of load group *j*.
$LF_{n,r,t}^{P}$ ($LF_{n,r,t,s}^{P}$)	Active power flow from node *n* to *r* in period *t* (and scenario *s*) (kW).
$LF_{n,r}^{\max}$	Maximum power flow from node *n* to *r* (kW).

$F^{Q}_{n,r,t}$ ($F^{Q}_{n,r,t,s}$)	Reactive power flow from node *n* to *r* in period *t* (and scenario *s*) (kVar).
$f_{t,s}$ ($\Delta f_{t,s}$)	MG frequency (excursion) at hour *t* and in scenario *s*.
$m_{p,i}$	Frequency droop control gain of DG *i*.
$G_{n,r}$ ($B_{n,r}$)	Conductance and susceptance of line that connected node *n* to node *r*.
M_x	Set of generating units *x* (load *x*) into the set of nodes.
$SDC_{i,t}$ ($SUC_{i,t}$)	Shut-down (start-up) cost of DG *i* in period *t* (cents).
$\rho_{j,t}$ ($\rho_{j,h}$)	Electricity price for load *j* in period *t* (in period *h*) (cents/kWh).
$\rho^{0}_{j,t}$ ($\rho^{0}_{j,h}$)	Initial electricity price for load *j* in period *t* (in period *h*) (cents/kWh).
$\rho^{Dep}_{j,t}$ ($\rho^{Dep}_{x,t}$)	Real-time price for buying and selling deviation power form load *j* (unit *x*) in period *t* (cents/kWh).
$P_{i,t}$ ($P_{i,t,s}$)	Scheduled power for DG *i* in period *t* (and scenario *s*) (kW).
$P_{w,t}$ ($P_{w,t,s}$)	Output power of WT *w* in period *t* (and scenario *s*) (kW).
$P_{v,t}$ ($P_{v,t,s}$)	Output power of PV *v* in period *t* (and scenario *s*) (kW).
$P^{\max}_{x}$ ($P^{\min}_{x}$)	Maximum (minimum) generating capacity of unit *x* (kW).
$P^{ref}_{i,t,s}$	Reference power set-point of DG *i* at hour *t* and in scenario *s*.
$R^{U}_{i,t}$ ($R^{U}_{j,t}$)	Scheduled up-spinning reserve for DG *i* (load *j*) in period *t* (kW).
$R^{D}_{i,t}$ ($R^{D}_{j,t}$)	Scheduled down-spinning reserve for DG *i* (load *j*) in period *t* (kW).
$R^{NS}_{i,t}$	Scheduled non-spinning reserve for DG *i* in period *t* (kW).
$r^{U}_{i,t,s}$ ($r^{U}_{j,t,s}$)	Up-spinning reserve deployed by DG *i* (load *j*) in period *t* and scenario *s* (kW).
$r^{D}_{i,t,s}$ ($r^{D}_{j,t,s}$)	Down-spinning reserve deployed by DG *i* (load *j*) in period *t* and scenario *s* (kW).
$r^{NS}_{i,t,s}$	Non-spinning reserve deployed by DG *i* in period *t* and scenario *s* (kW).
$L^{shed}_{j,t,s}$	Inelastic load shedding level of *j-th* load group in period *t* and scenario *s* (kW).
$\delta_{n,t}$ ($\delta_{n,t,s}$)	Voltage angle at node *n* in period *t* (and scenario *s*) (rad).
$V_{n,t}$ ($V_{n,t,s}$)	Voltage magnitude (RMS value) at node *n* in period *t* (and scenario *s*) (p.u.).
$u_{i,t}$ ($u_{i,t,s}$)	Binary variable, equal to 1 if unit *i* is scheduled to be committed in period *t* (and scenario *s*), otherwise 0.
$y_{i,t}$ ($y_{i,t,s}$)	Binary variable, equal to 1 if unit *i* is starting up in period *t* (and scenario *s*), otherwise 0.
$z_{i,t}$ ($z_{i,t,s}$)	Binary variable, equal to 1 if unit *i* is shut down in period *t* (and scenario *s*), otherwise 0.
Λ	Set of lines.
η_j	The potential of DR programs implementation by load *j*.
π_s	Probability of scenario *s*.

I. Introduction

Recently, microgrid (MG) idea has been introduced to transform the conventional power systems to a more reliable, economic and environmentally friendly system. The diversified load consumption pattern and availability of power from green distributed energy resources (DERs) cause supply–demand mismatch in MGs. Optimal operation of MGs both technically and economically mainly relies on the coordination between different components including DERs, energy storage systems (ESSs), and responsive loads [1]-[2]. In grid-connected MGs, normally the economic operation is the main objective as there is a stiff-grid on upstream to support the system frequency and voltage at the point of common coupling. However, in islanded mode, the economic operation is rather inferior as the main goal is to provide an uninterruptible power supply with appropriate quality to the loads [3]. Therefore, in both operating modes, a proper energy management system (EMS) is required to adjust the active and reactive power set-points for the dispatchable

DERs to feed the total load and to meet the MG economic targets [4]-[6]. If the renewable energy sources (RESs) such as wind and solar power contribute significantly in the supply side, the deviation in the forecast of renewables can adversely affect the reliable operation of the MG. Therefore, to properly balance power generation and consumption, efficient mechanisms for reliable system operation in the presence of uncertainties imposed by stochastic behavior of energy sources is needed. With active participation of end-use consumers in demand response (DR) programs, it is very probable to compensate power mismatch in an islanded MG [7]-[8]. The positive impact of DR on the operation and costs of MGs has been studied in the literature [8]-[13]. Participation of customers in DR programs could greatly improve the system reliability and stability, reduce the total system operating costs, shape the daily load profile and provide financial incentives to the customers to benefit from lower hourly demands. However, optimal scheduling of responsive loads and DERs in islanded MGs under uncertainties with considering system security is a more important problem that needs to be quantified and better examined.

The energy management strategies in isolated MGs considering impact of DR on their operation and costs has been analyzed in a number of research works [15]-[17]. For example, in [14], a DR scheduling model is presented for the novel residential community incorporating the current circumstances and the future trends of DR programs. In this study, at first, residential loads are classified into different categories according to various DR programs and then a complete scheduling scheme is modeled based on the dispatch of residential loads and distributed generation. In [15], an EMS is proposed for MGs where the main objective is to minimize the system cost as well as meeting the demand. The uncertainties of RESs and DR participation are also taken into account. Authors in [16] present a stochastic programming model for the optimal operation scheduling of DER with renewable resources considering economic and environmental aspects. In this study, a trade-off solution is obtained for operator based on economic and environmental priorities under uncertainties in demand and supply sides. In [17], a stochastic programming model is proposed to optimize the performance of a MG in a short term to minimize operating costs and emissions with renewable sources. In the same study, the authors use incentive-based payments as price offer packages in order to implement DR programs. In [18], a daily optimal scheduling problem of MGs considering intermittent behavior in generation and demand is investigated, where two DR programs based on time of use (TOU) and real time pricing (RTP) are integrated into the optimal scheduling model.

In the above-mentioned references that have addressed the MG scheduling with considering DR participants, the MG security issues are not studied. However, some other works tackle the problem of optimal energy resources and demand-side scheduling with considering system security issues [19]-[23]. For example, a stochastic multi-objective framework is proposed in [19] for joint energy and reserve scheduling in day-ahead, however this reference does not consider AC network, voltage security, load and wind power uncertainties. In [20], a security-constrained energy management is presented with considering the steady-state frequency response of the MG. Moreover, the authors investigate the effect of DR participants on frequency security as a linearized ancillary service of DR programs. In [21] a cost-effective frequency-dependent energy management system is presented and the role of primary and secondary reserve resources on steady-state frequency-security is investigated accordingly. In the same work, the authors only concentrate on static performance of DERs and the effect of DR participants on voltage and frequency security is not considered. Likewise, an energy management strategy is proposed in [22] to coordinately manage the generating units and DR resources in a MG such that both static and dynamic frequency security constraints are met, however, the effect of DR participants on voltage security is not investigated. A control framework for the participation of responsive loads in the voltage and frequency control of a given MG is proposed in [23]. Moreover, a hierarchical energy management framework for the coordination of DER units and DR for voltage and frequency support of islanded MGs is introduced in [24]. The proposed methods in this reference relies on extracting information from real and reactive power sensitivities at different buses for minimizing the voltage and frequency deviations of islanded MGs; however, the effect of various uncertainties on system security is not considered. Also, a novel EMS is presented in [25] to efficiently procure the frequency security requirements of an islanded MGs. The main objective of the proposed model in this reference is to optimize the MG frequency security and also the rate of change of frequency indices by providing a sustainable strategy for managing the energy and reserve resources.

This paper addresses a security-constrained energy and reserve scheduling problem, in which DR participants along with the DERs in the islanded MG are scheduled optimally in an uncertain environment. In this regard, a two-stage stochastic optimization model is developed for optimal scheduling of energy-related consumption and production units in a way to meet the maximum profit of MGO under the premise frequency and voltage security constraints. In the proposed model customers are able to participate in reserve market under DR programs and their behavioral uncertainties are modeled properly. In this study, different schemes of DR based on TOU pricing are also investigated and their effects on the voltage and frequency regulations in a residential islanded MG are studied. In this work, different schemes of DR based on TOU pricing are also investigated and their effects on the voltage and frequency regulations in a residential islanded MG are studied. As an extension of the concepts developed in prior works, the

proposed framework of this paper also applies AC-optimal power flow (AC-OPF) in each working condition to ensure the validity of solution in terms of voltage and frequency security. In addition, in this study the sensitivity of the profit and the system security margin in cases with and without DR participants are studied.

Compared to the recent works in this area, a number of contributions have been in this work. First, a proper model of responsive loads is developed to analyze the effect of customers' participation in DR programs on economy and security of an islanded MG. In this model customers participate in DR using two general categories of electrical devices including sheddable and shiftable loads. Unlike the previous works, the locations of the loads in the MG are also considered in our study which results in more accurate analysis. As mentioned earlier, most of the recent works use DC-power flow methodologies in connection with their optimization problems which in turn neglect reactive power flows and their impact on nodal voltages and system frequency. However, in our suggested approach, the frequency and bus voltage deviations are determined accurately using AC-OPF methodologies. Moreover, in this work, the effect of DR participation levels on voltage and frequency regulation is investigated. To clearly demonstrate the contributions of this work, Table 1 represents a systematically comparison between the performance of our proposed approach and those of the recent works in the same subject area. As it can be seen in the reviewed literature [15]-[24], the reactive power dispatch problem has been easily neglected and the DC-OPF methodology has mainly been used in connection with the proposed optimization problems. Moreover, as an extension of the concepts developed in prior works (e.g.,[25] [24], [25]) where the effect of various uncertain parameters on the system security has not been considered, in this paper, uncertainties of renewable resources and responsive loads are modelled properly. As a whole, the contributions of this work can be highlighted as:

1- Optimal coordination of DERs and responsive loads is presented with considering customers' participation in TOU-DR program,
2- Simultaneous energy and reserve scheduling is proposed with regard to maximum expected profit of MGO under the premise of security and stability of MGs in an uncertain environment,
3- An AC-OPF approach is applied to model the actual operating conditions and to assess the influence of DR resources on voltage and frequency security.

Table 1. A systematical comparison between the contribution of recent works and this paper.

Option	Ref. / Type	[14]	[15], [16]	[17], [18]	[19], [20]	[21], [23]	[24], [25]	Proposed Model
DR Participants	in Energy Scheduling	YES	YES	YES	YES	YES	YES	YES
	in Reserve Provision	NO	YES	YES	YES	YES	YES	YES
Security Constraints	System Frequency	NO	NO	NO	YES	YES	YES	YES
	Bus Voltage	NO	NO	NO	NO	NO	YES	YES
Uncertainty	RESs	NO	YES	YES	YES	YES	NO	YES
	DR	NO	YES	YES	NO	YES	NO	YES
Power Dispatch	Active Power	YES	YES	YES	YES	YES	YES	YES
	Reactive Power	NO	NO	NO	NO	NO	YES	YES
	Power Flow Type	DC-OPF	DC-OPF	DC-OPF	DC-OPF	DC-OPF	AC-OPF	AC-OPF

The organization of the paper is as follows: section II describes the model description and formulation and the case studies and discussion about the simulation results are given in Section III. Findings of this work are summarized in Section IV.

II. Model Description and Formulation

A. Model description

The process of investigating DERs and DR impact on security-constrained energy and reserve scheduling from the MGO's perspective is shown in Fig. 1. Based on this structure, DERs including dispatchable distributed generations (DGs) and renewable resources and also responsive loads should be managed in a way not only to satisfy the system's objectives, but also to meet the technical/security constraints. In this process, MGO plays the key role as it monitors the optimal scheduling process and has a supervisory on decisions. For effective DR enabling, it is assumed that the

customers are equipped with house energy management controllers and several residential smart appliances. Moreover, it is assumed that customers of different characteristics (based on their location in the network and their participation level in DR programs) are categorized into N_j groups and $\%\eta_j$ of customers at each group sign contracts to participate in DR programs. Other required information such as RESs available power and customers demand are predicted using predication methods.

The MGO solves the security-constrained energy and reserve scheduling problem over the scheduling time horizon to find the optimal solution with regard to system objectives which are defined as maximization of the MGO profit and minimization of the customer's payment.

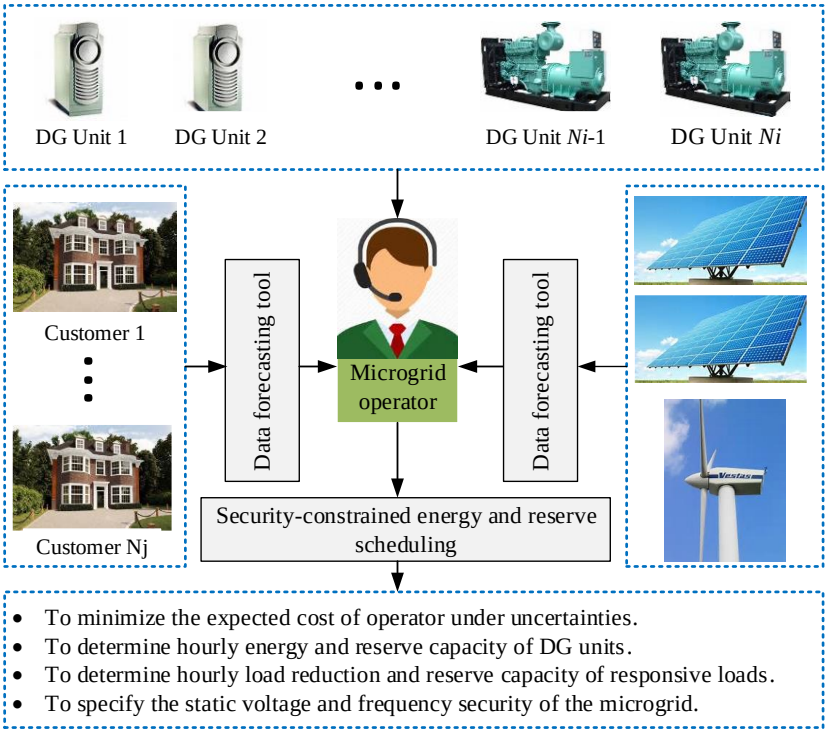

Fig. 1. The proposed framework for security-constrained energy and reserve scheduling from MGO's perspective.

B. Proposed solution methodology

Framework of the proposed solution methodology is presented in Fig. 2. The input data to the proposed structure consists of two categories, deterministic data and stochastic data which are obtained by modelling as random processes. Because of the stochastic consideration for wind and PV generation and also loads consumption, at first, some scenarios are generated based on probability density functions (PDFs). Then, by implementing an efficient scenario reduction algorithm, N_S scenarios are selected that represents well enough the uncertainties. In the next step, the reduced scenarios are applied to the proposed MIP-based optimization model to maximize the expected profit of islanded MGO while considering system voltage and frequency security constraints. As it can be seen from flowchart, the proposed scheduling problem consists of master problem and sub-problems that use Benders decomposition (BD) theory to get the solutions [27]. In the master problem, unit commitment (UC) and the status of DG units, economic dispatch and also the amount LC/LS in DR programs are determined in a MIP problem. Sub-problem solves, instead, a 24-h Nonlinear Programming Problem (NLP) representing hourly AC security-constrained OPF. The solution generated by the upper layer (master problem) is considered in the sub-problem and the feasibility and optimality of the optimal decision of base case decisions is evaluated under system contingencies to detect flow violations. If sub-problem fails to get a feasible solution, accordingly an infeasibility cut based on the BD theory is created and included to the master problem to recalculate the dispatch and hourly commitment states of the generating units and also responsive loads condition.

A. Uncertainty modeling of renewable resources and electric demand

In order to model the variation of wind power generation, the historical data records of wind speed, v, is used and modeled by Rayleigh PDF [22]. The general Rayleigh PDF for wind speed can be formulated as follows [27]:

$$PDF(v) = (\frac{v}{c^2}).\exp\left[-(\frac{v^2}{2c^2})\right] \quad (1)$$

where, v, k and c are wind speed, shape factor (dimensionless) and scale factor, respectively. Besides, the output power of WT can be described by Eq. (18) [22] :

$$P_w(v) = \begin{cases} 0 & ; 0 \le v \le v_{in} \quad or \quad v \ge v_{out} \\ (\frac{v - v_{in}}{v_r - v_{in}}).P_w^r & ; v_{in} \le v \le v_r \\ P_w^r & ; v_r \le v \le v_{out} \end{cases} \quad (2)$$

where, v_r, v_{in} and v_{out} indicate the rated speed, cut-in speed and cut-out speed of the WT, respectively, and P_w^r represents the total rated power of WT.

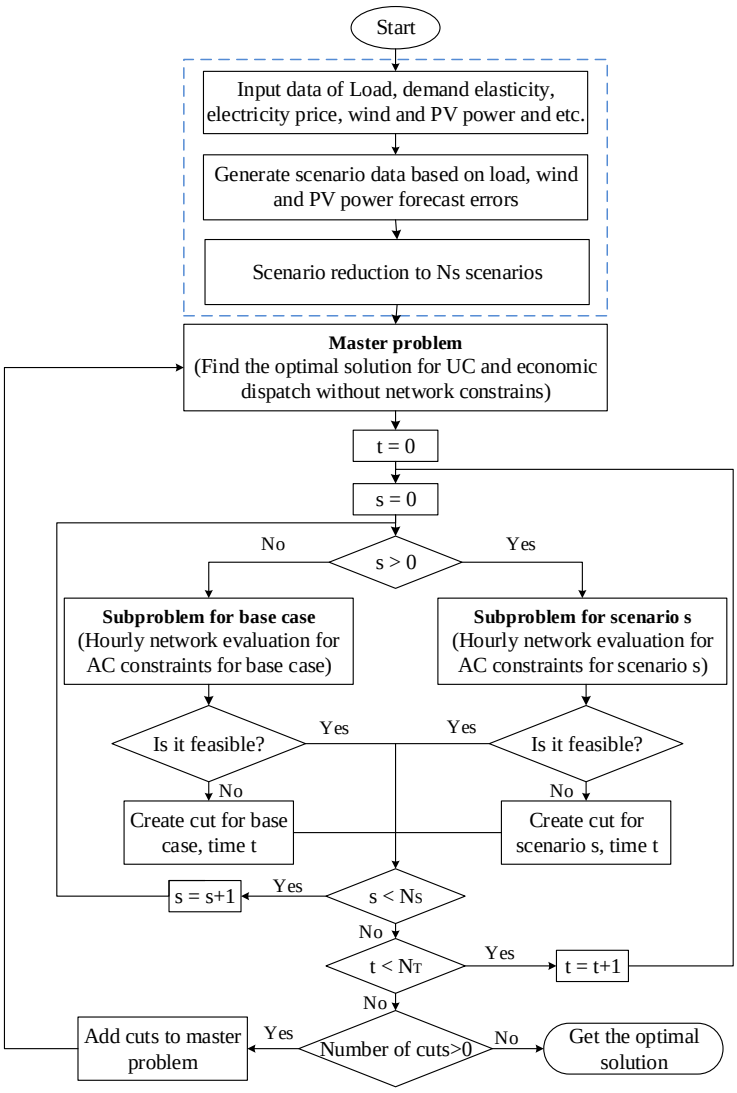

Fig. 2. Flowchart of the proposed scheduling algorithm.

The distribution of hourly irradiance usually follows a bimodal distribution, which can be seen as a linear combination of two unimodal distribution functions [29]. A Beta PDF is utilized for each unimodal, as stated in the following:

$$f_b(\varphi)=\begin{cases}\dfrac{\Gamma(\alpha+\beta)}{\Gamma(\alpha).\Gamma(\beta)}.\varphi^{(\alpha-1)}\times(1-\varphi)^{\beta-1} & ;\quad 0\le\varphi\le 1,\ \alpha\ge 0,\ \beta\ge 0\\ 0 & ;\quad otherwise\end{cases} \tag{3}$$

The parameters of the Beta distribution function (α , β) are calculated based on the mean (μ) and standard deviation (σ) of the random variable as follows:

$$\alpha=\frac{\mu\times\beta}{1-\mu},\quad \beta=(1-\mu)\times\left(\frac{\mu\times(1+\mu)}{\sigma^2}-1\right) \tag{4}$$

Additionally, the uncertainties of load and demand elasticity are considered as stochastic variables and their forecasting errors are modeled using normal distribution function with a known mean and variance. In this study, to model the uncertainties of each stochastic variable, a set of possible scenarios are generated based on Metropolis–Hastings algorithm using related PDFs. Then generated scenarios are reduced into an optimal subset that represents well enough the uncertainties using the *k*-means clustering technique [30]. Finally, the scenarios are combined to construct the whole set of scenarios based on a scenario tree [31]. Each branch in scenario tree corresponds to one scenario in scheduling horizon with a probability calculated as follows:

$$\pi_s=\pi_{ws}\times\pi_{vs}\times\pi_{ls} \tag{5}$$

where π_{ws} , π_{vs} and π_{ls} are the probabilities of the ws^{th} wind, vs^{th} PV and ls^{th} load scenarios, respectively.

B. AC- Power flow constraints

In an islanded MG, the frequency and the voltage are affected by any active and reactive power mismatches between the generation and the consumption side. Thus, an AC-power flow is required to calculate the voltages and frequency deviations in the absence of an infinite bus. The active and reactive power balance equations in the time interval *t* in each bus of MG in steady state are defined as:

$$\sum_{i:(i,n)\in M_I(t)}P_{i,t}+\sum_{w:(w,n)\in M_W(t)}P_{w,t}+\sum_{v:(v,n)\in M_V(t)}P_{v,t}-\sum_{j:(j,n)\in M_L(t)}D_{j,t}=\sum_{r:(n,r)\in\Lambda(t)}LF^{P}_{n,r,t} \tag{6}$$

$$\sum_{i:(i,n)\in M_I(t)}Q_{i,t}+\sum_{w:(w,n)\in M_W(t)}Q_{w,t}+\sum_{v:(v,n)\in M_V(t)}Q_{v,t}-\sum_{j:(j,n)\in M_L(t)}Q_{j,t}=\sum_{r:(n,r)\in\Lambda(t)}LF^{Q}_{n,r,t} \tag{7}$$

where $f^{P}_{n,r,t}$ and $f^{Q}_{n,r,t}$ are considered as active and reactive power flow from bus *n* to bus *r* at time interval *t*, respectively and calculated as follow:

$$LF^{P}_{n,r,t}=G_{n,r}\left[V^2_{n,t}-V_{n,t}.V_{r,t}\cos(\delta_{n,t}-\delta_{r,t})\right]-B_{n,r}V_{n,t}.V_{r,t}\sin(\delta_{n,t}-\delta_{r,t}) \tag{8}$$

$$LF^{Q}_{n,r,t}=-B_{n,r}\left[V^2_{n,t}-V_{n,t}.V_{r,t}\cos(\delta_{n,t}-\delta_{r,t})\right]-G_{n,r}V_{n,t}.V_{r,t}\sin(\delta_{n,t}-\delta_{r,t}) \tag{9}$$

There are several operating constraints for DG units that represent the relationship between active power productions of DGs and upward/downward regulation capacities as follows:

$$P_i^{\min}u_{i,t}+R^{D}_{i,t}\le P_{i,t}\le P_i^{\max}u_{i,t}-R^{U}_{i,t} \tag{10}$$

$$0\le R^{U}_{i,t}\le R^{U,\max}_{i,t}u_{i,t} \tag{11}$$

$$0\le R^{D}_{i,t}\le R^{D,\max}_{i,t}u_{i,t} \tag{12}$$

$$0\le R^{NS}_{i,t}\le R^{NS,\max}_{i,t}(1-u_{i,t}) \tag{13}$$

The same technical/operating conditions must be met for the system in each working scenario as follows:

$$\sum_{i:(i,n)\in M_I(t,s)} P_{i,t,s} + \sum_{w:(w,n)\in M_W(t,s)} P_{w,t,s} + \sum_{v:(v,n)\in M_V(t,s)} P_{v,t,s} - \sum_{j:(j,n)\in M_L(t,s)} (D_{j,t,s} - L^{shed}_{j,t,s}) = \sum_{r:(n,r)\in\Lambda(t,s)} LF^{P}_{n,r,t,s} \quad (14)$$

$$\sum_{i:(i,n)\in M_I(t,s)} Q_{i,t,s} + \sum_{w:(w,n)\in M_W(t,s)} Q_{w,t,s} + \sum_{v:(v,n)\in M_V(t,s)} Q_{v,t,s} - \sum_{j:(j,n)\in M_J(t,s)} (Q_{j,t,s} - Q^{shed}_{j,t,s}) = \sum_{r:(n,r)\in\Lambda(t,s)} LF^{Q}_{n,r,t,s} \quad (15)$$

$$LF^{P}_{n,r,t,s} = G_{n,r}\left[V^2_{n,t,s} - V_{n,t,s}.V_{r,t,s}\cos(\delta_{n,t,s} - \delta_{r,t,s})\right] - B_{n,r}V_{n,t,s}.V_{r,t,s}\sin(\delta_{n,t,s} - \delta_{r,t,s}) \quad (16)$$

$$LF^{Q}_{n,r,t,s} = -B_{n,r}\left[V^2_{n,t,s} - V_{n,t,s}.V_{r,t,s}\cos(\delta_{n,t,s} - \delta_{r,t,s})\right] - G_{n,r}V_{n,t,s}.V_{r,t,s}\sin(\delta_{n,t,s} - \delta_{r,t,s}) \quad (17)$$

Equations (14)-(17) describe the AC power flow constraints in real-time operation of MG that guarantee the balance of the active and reactive powers at different nodes. When the frequency deviates from its nominal values, MG central controller (MGCC) must restore that to the reference value by readjusting the active power set-points of dispatchable DG units and/or enabling DR actions. Moreover, the restoration function should be activated inline with the MG economic objectives. Therefore, based on the performances of the droop controlled of DGs [32], the stay-state frequency deviation can be formulated by (18):

$$\Delta f_{t,s} = -\sum_{i}^{N_G}(P_{i,t,s} - P^{ref}_{i,t,s}) / [D_{L,t,s} + \sum_{i}^{N_G}(\frac{1}{m_{p,i}})u_{i,t}] \quad (18)$$

where, $D_{L,t,s}$ is the frequency elasticity of MG loads at period *t* and in scenario *s*. In other to keep the frequency stable, MGCC has to regulate the active power generation of DG units so as to meet the following criterion:

$$\left|\Delta f_{t,s}\right| \le \Delta f^{\max} \quad (19)$$

where, $\Delta f^{\max}$ is the maximum value of MG frequency excursion. Equations (20)-(21) represent the linear models for the startup cost of DG units.

$$SUC_{i,t,s} \ge \lambda^{SU}_{i,t}(u_{i,t,s} - u_{i,t-1,s}) \quad (20)$$

$$SUC_{i,t,s} \ge 0 \quad (21)$$

Constraints (22)-(23) couple the first stage decisions with possible realizations of stochastic processes. Equation (22) represents the relationship between the scheduled power of DGs and their deployed powers and reserves in scenarios. Also, Equation (23) stipulates the relationship between the scheduled values of load and deployed energy and reserves in the scenarios for each group of customers.

$$P_{i,t} = P_{i,t,s} + r^{U}_{i,t,s} + r^{NS}_{i,t,s} - r^{D}_{i,t,s} \quad (22)$$

$$L_{j,t} = L_{j,t,s} - r^{U}_{j,t,s} + r^{D}_{j,t,s} \quad (23)$$

Constraints (24)-(25) represent the WT and PV power production limit, respectively.

$$0 \le P_{w,t,s} \le P^{\max}_{w} \quad (24)$$

$$0 \le P_{v,t,s} \le P^{\max}_{v} \quad (25)$$

The relationship between the active power production limits of DG units and generation-side reserve and DGs deployed reserves limits are represented by (26)-(29).

$$P^{\min}_{i}u_{i,t,s} + R^{D}_{i,t,s} \le P_{i,t,s} \le P^{\max}_{i}u_{i,t,s} - R^{U}_{i,t,s} \quad (26)$$

$$0 \le r_{i,t,s}^{U} \le R_{i,t,s}^{U} \tag{27}$$

$$0 \le r_{i,t,s}^{D} \le R_{i,t,s}^{D} \tag{28}$$

$$0 \le r_{i,t,s}^{NS} \le R_{i,t,s}^{NS} \tag{29}$$

Moreover, (30)-(34) present the constraints on nodal voltages, line power flows, emergency load curtailments and reactive powers, respectively.

$$-V_n^{\min} \le V_{n,t,s} \le V_n^{\max} \tag{30}$$

$$\sqrt{\left(LF_{n,r,t,s}^{P}\right)^2 + \left(LF_{n,r,t,s}^{Q}\right)^2} \le LF_{n,r}^{\max} \tag{31}$$

$$Q_i^{\min} \le Q_{i,t,s} \le Q_i^{\max} \tag{32}$$

$$0 \le L_{j,t,s}^{shed} \le L_{j,t} \tag{33}$$

$$Q_{j,t,s}^{shed} = \cos\theta . L_{j,t,s}^{shed} \tag{34}$$

Constraints (35)-(36) stand for the up- and down-deployed reserves limits of the demand-side. It should be noted that the up-reserves deployed by the demand-side is defined as a decrease in the consumption level, while down-reserve is defined oppositely.

$$0 \le r_{j,t,s}^{U} \le R_{j,t,s}^{U} \tag{35}$$

$$0 \le r_{j,t,s}^{D} \le R_{j,t,s}^{D} \tag{36}$$

C. Demand Response Model

Consumers participate in DR programs and change their consumption patterns over the time based on the electricity price signals. Therefore, the total demand after load participation in DR program at each time interval *t* can be calculated as:

$$D_t = \sum_{j=1}^{N_J} \left[D_{j,t}^{NDR} + D_{j,t}^{DR} \right] \tag{37}$$

where, $D_{j,t}^{NDR}$ and $D_{j,t}^{DR}$ represent the non-responsive and responsive loads of group *j* of customers at time interval *t*, respectively. To achieve the maximum benefit, each group of customers may change the load level from $D_{j,t}$ to $D_{j,t}^{DR}$ in period *t*, as:

$$D_{j,t}^{DR} = D_{j,t} + \Delta D_{j,t}^{DR} \tag{38}$$

where, $\Delta D_{j,t}^{DR}$ is load changes due to DR participants. The benefit of group *j* of customers can be obtained as:

$$S(D_{j,t}^{DR}) = B(D_{j,t}^{DR}) - D_{j,t}^{DR} . \rho_{j,t} \tag{39}$$

where, $S(D_{j,t}^{DR})$ and $B(D_{j,t}^{DR})$ represent benefit and income of group *j* at period *t* after implementing DR programs, respectively. In order to maximize the benefit of group *j*, (40) must be met,

$$\frac{\partial S(D_{j,t}^{DR})}{\partial D_{j,t}^{DR}} = \frac{\partial B(D_{j,t}^{DR})}{\partial D_{j,t}^{DR}} - \rho_{j,t} = 0 \Rightarrow \frac{\partial B(D_{j,t}^{DR})}{\partial D_{j,t}^{DR}} = \rho_{j,t} \tag{40}$$

The changes in demand due to change in price at the same time instant *t* is defined as self-elasticity [1], and can be mathematically represented as follows:

$$E_{j,t,t} = \frac{\rho_{j,t}^0}{D_{j,t}^0}.\frac{\partial D_{j,t}}{\partial \rho_{j,t}} \tag{41}$$

By using Eq. (41) and based on the quadratic model of DR, the income of group *j* of customer at period *t* after implementing DR programs is obtained as:

$$B(D_{j,t}^{DR}) = B_{j,t}^0 + \frac{\rho_{j,t}^0.D_{j,t}^{DR}}{1+E_{j,t,t}^{-1}} \times \left[(\frac{D_{j,t}^{DR}}{D_{j,t}})^{E_{j,t,t}^{-1}} - 1 \right] \tag{42}$$

Differentiating (42) with respect to $D_{j,t}^{DR}$ yields:

$$\frac{\partial B(D_{j,t}^{DR})}{\partial D_{j,t}^{DR}} = \frac{\rho_{j,t}^0}{1+E_{j,t,t}^{-1}} \times \left[(\frac{D_{j,t}^{DR}}{D_{j,t}})^{E_{j,t,t}^{-1}} - 1 \right] + \frac{\rho_{j,t}^0.D_{j,t}^{DR}}{1+E_{j,t,t}^{-1}} \times \left[E_{j,t,t}^{-1}.\frac{1}{D_{j,t}} (\frac{D_{j,t}^{DR}}{D_{j,t}})^{E_{j,t,t}^{-1}-1} \right] \tag{43}$$

Substituting (43) into (40) gives:

$$(1+E_{j,t,t}^{-1}) \times \frac{\rho_{j,t}^0}{\rho_{j,t}} = (\frac{D_{j,t}^{DR}}{D_{j,t}})^{E_{j,t,t}^{-1}} - 1 + E_{j,t,t}^{-1}.(\frac{D_{j,t}^{DR}}{D_{j,t}})^{E_{j,t,t}^{-1}} \Rightarrow \frac{\rho_{j,t}}{\rho_{j,t}^0} = (\frac{D_{j,t}^{DR}}{D_{j,t}})^{E_{j,t,t}^{-1}} - \frac{1}{1+E_{j,t,t}^{-1}} \tag{44}$$

Therefore, the consumption of group *j* at time t is obtained as follows:

$$D_{j,t}^{DR} = D_{j,t}.(\frac{\rho_{j,t}}{\rho_{j,t}^0} + \frac{1}{1+E_{j,t,t}^{-1}})^{E_{j,t,t}} \tag{45}$$

In a like manner, cross-elasticity is defined as demand sensitivity of the t^{th} period with respect to the price elasticity at h^{th} period [13] and can be mathematically formulated as follows:

$$E_{j,t,h} = \frac{\rho_{j,h}^0}{D_{j,t}^0}.\frac{\partial D_{j,t}}{\partial \rho_{j,h}} \tag{46}$$

Based on the quadratic model of DR and using Eq.(46), responsive loads that shifted from another period to period *t* are modeled as:

$$D_{j,t}^{DR} = D_{j,t}.\exp\left[\sum_{\substack{h=1 \\ h\neq t}}^{N_T} E_{j,t,h}.\ln(\frac{\rho_{j,h}}{\rho_{j,h}^0} + \frac{1}{1+E_{j,t,h}^{-1}}) \right] \tag{47}$$

$$D_{j,t}^{DR} = D_{j,t}.\prod_{\substack{h=1 \\ h\neq t}}^{N_T} (\frac{\rho_{j,h}}{\rho_{j,h}^0} + \frac{1}{1+E_{j,t,h}^{-1}})^{E_{j,t,h}} \tag{48}$$

Therefore, the customers' total loads after participating in DR programs is obtained with the summation of (45) and (48) as follows:

$$\begin{aligned} D_{j,t}^{DR} = D_{j,t}.\prod_{h=1}^{N_T} \left(\frac{\rho_{j,h}}{\rho_{j,h}^0} + \frac{1}{1+E_{j,t,h}^{-1}} \right)^{E_{j,t,h}} &\Rightarrow D_{j,t}^{DR} = D_{j,t}.\prod_{h=1}^{N_T} \exp\left[\ln\left(\frac{\rho_{j,h}}{\rho_{j,h}^0} + \frac{1}{1+E_{j,t,h}^{-1}} \right)^{E_{j,t,h}} \right] \\ \Rightarrow D_{j,t}^{DR} = D_{j,t}.\exp\sum_{h=1}^{N_T} E_{j,t,h}.\ln&\left(\frac{\rho_{j,h}}{\rho_{j,h}^0} + \frac{1}{1+E_{j,t,h}^{-1}} \right) \end{aligned} \tag{49}$$

By replacing (49) into (37), the load economic model is obtained as:

$$D_{j,t} = (1-\eta_j)D_{j,t} + \eta_j.D_{j,t}.\exp\sum_{h=1}^{N_T} E_{j,t,h}.\ln(\frac{\rho_{j,h}}{\rho_{j,h}^0} + \frac{1}{1+E_{j,t,h}^{-1}}) \tag{50}$$

It is should be noted that both active and reactive loads can be modeled taking into account their voltage and frequency dependence so that the amount of total active and reactive load of bus *n* at time interval *t* and scenario *s* can be obtained as [23]:

$$D_{j,t,s} = \overline{D}_{j,t}.(1+k_{pj}\Delta f_{t,s}).\left[(p_{pj} + p_{cj}(\frac{V_n}{V_n^*}) + p_{zj}(\frac{V_n}{V_n^*})^2 \right] \tag{51}$$

$$Q_{j,t,s} = \overline{Q}_{j,t}.(1+k_{qj}\Delta f_{t,s}).\left[(q_{pj} + q_{cj}(\frac{V_n}{V_n^*}) + q_{zj}(\frac{V_n}{V_n^*})^2 \right] \tag{52}$$

where, $\overline{D}_{j,t}$ and $\overline{Q}_{j,t}$ are respectively the specified active and reactive loads of group *j* of customers at period *t*, k_{pj} and k_{qj} denote the coefficients of the frequency characteristics of the load, and p_{pj}, p_{cj}, p_{zj}, q_{pj}, q_{cj} and q_{zj} stand for the coefficients of the voltage characteristics of loads of group *j*. Moreover, V_n^* is voltage magnitude (RMS value) associated with $\overline{D}_{j,t}$ and $\overline{Q}_{j,t}$ .One can use appropriate values for the mentioned coefficients to model different types of load [33].

The demand-side constraints determine the degree of participation of each group of customers in energy and reserve scheduling. These constraints for both of active and reactive demand loads are given as:

$$D_{j,t}^{\min} \le D_{j,t} \le D_{j,t}^{\max} \tag{53}$$

$$0 \le R_{j,t}^{U} \le D_{j,t} - D_{j,t}^{\min} \tag{54}$$

$$0 \le R_{j,t}^{D} \le D_{j,t}^{\max} - D_{j,t} \tag{55}$$

D. Objective function

The objective function is to maximize the total profit of the MGO during the scheduling time horizon. The profit of MGO includes the revenue of selling energy to customers minus the costs of energy and reserve provision as well as the expected costs of operation under uncertainties. In this regard the problem of optimal DER and DR scheduling can be formulated as an optimization problem with the following objective and a set of constraints described earlier.

$$\begin{aligned} Max\Bigg\{ & \Bigg[\sum_{t=1}^{N_T}\sum_{j=1}^{N_J} \rho_{j,t}.D_{j,t} \\ & - \sum_{t=1}^{N_T}\sum_{i=1}^{N_G} \Big[(A_i.u_{i,t} + B_i.P_{i,t}) + SUC_i.y_{i,t} + SDC_i.z_{i,t} \\ & + (C_{i,t}^{R^D}.R_{i,t}^{D} + C_{i,t}^{R^U}.R_{i,t}^{U} + C_{i,t}^{R^{NS}}.R_{i,t}^{NS}) \Big] \\ & + (C_{j,t}^{R^D}.R_{j,t}^{D} + C_{j,t}^{R^U}.R_{j,t}^{U}) \\ & - \sum_{t=1}^{N_T} \Bigg[\sum_{w=1}^{N_W} \rho_{w,t}.P_{w,t} + \sum_{v=1}^{N_V} \rho_{v,t}.P_{v,t} \Bigg] \\ & \Bigg] - \Bigg[\\ & \sum_{s=1}^{N_S}\sum_{t=1}^{N_T}\sum_{i=1}^{N_G} \pi_s.\Big[SUC_i.(y_{i,t,s} - y_{i,t}) + \\ & SDC_i.(z_{i,t,s} - z_{i,t}) - \rho_{i,t}^{Dep}.(r_{i,t,s}^{U} + r_{i,t,s}^{NS} - r_{i,t,s}^{D}) \Big] \\ & \sum_{s=1}^{Ns}\sum_{t=1}^{T} \Bigg[\pi_s.\sum_{j=1}^{N_J} \rho_{j,t}^{Dep}.(r_{j,t,s}^{U} - r_{j,t,s}^{D}) \\ & \sum_{s=1}^{N_S}\sum_{t=1}^{N_T} \Bigg[\pi_s.\sum_{w=1}^{N_W} \rho_{w,t}^{Dep}.\Delta P_{w,t,s} + \sum_{v=1}^{N_V} \rho_{v,t}^{Dep}.\Delta P_{v,t,s} \Bigg] \\ & \sum_{j=1}^{N_J} VOLL.EENS_j \Bigg\} \Bigg] \Bigg\} \end{aligned} \tag{56}$$

In (56) the first line represents the MGO's revenue from selling electricity to the customers. The second line is the cost of DG units and their start-up and shut-down costs. The third line represents the costs of scheduled reserve of generating units and responsive loads. The fourth line represents the cost of energy that the MGO purchases from the WT and PV owners. In this study, it is assumed that the WT and PV units are not owned by the MGO, and so, the WT and PV sell their energy to the MGO based on specified prices. The fifth line denotes the costs of unit commitment in different scenarios. The sixth line denotes the costs of deploying reserves from DGs and responsive loads. The seventh line stands for the cost of power provision by WT and PV units that stems from the deviation between the real-time power output and the day-ahead forecasted power. It should be noted that in the first stage of scheduling, MGO schedules WT and PV units based on their forecasted values. But, due to variable climate, the output power of WT and PV units changes always. Therefore, the real-time output power may differ from day-ahead forecasted power. In fact, the seventh line represents the exchanged cost that should be paid to (obtained from) the WT and PV units' owners based on the difference between their forecasted and actual power production in scenarios. Therefore, this term can be positive or negative in the scheduling time horizon. Finally, the last line represents the cost of expected energy not served (EENS) for the inelastic loads at different scenarios. The amount of EENS for consumer *j* during the scheduling horizon can be calculated as follows:

$$EENS_j = \sum_{t=1}^{N_T}\sum_{s=1}^{N_S} \pi_s . L_{j,t,s}^{shed} \tag{57}$$

where, $L_{j,t,s}^{shed}$ is the mandatory load shedding imposed on consumers of group *j* in period *t* and scenario *s*.

E. Piecewise Linear AC Power Flow

In the above formulation, AC power flow constraints are nonlinear and should be linearized to be appropriate for linear programming model. Equations (58) and (59) present a piecewise linear approximation to AC power flow, in which voltage and reactive power are modeled as [34]:

$$f_{n,r,t,s}^{P} = G_{n,r}(V_{n,t,s} - V_{n,t,s} - \omega_{n,r,t,s} + 1) - B_{n,r}(\delta_{n,t,s} - \delta_{r,t,s}) \tag{58}$$

$$f_{n,r,t,s}^{Q} = -B_{n,r}(V_{n,t,s} - V_{n,t,s} + \omega_{n,r,t,s} + 1) - G_{n,r}(\delta_{n,t,s} - \delta_{r,t,s}) \tag{59}$$

Over a typical range of voltage angle, i.e., $\left|\delta_{n,t,s} - \delta_{r,t,s}\right| \le 10^{\circ}$, $\omega_{n,r,t,s}$ represents the piecewise linear approximation of $\cos(\delta_{n,t,s} - \delta_{r,t,s})$ that is [34].

$$\omega_{n,r,t,s} = d_{n,r,t,s,m} . (\delta_{n,t,s} - \delta_{r,t,s}) + e_{n,r,t,s,m} \tag{60}$$

where, $d_{n,r,t,s,m}$ and $e_{n,r,t,s,m}$ are chosen so that $\omega_{n,r,t,s}$ and $\cos(\delta_{n,t,s} - \delta_{r,t,s})$ intersect at break points. The approximation errors associated with this model can be found in [35].

III. Simulation and Results

The single line diagram of a typical low-voltage MG involving three radial feeders is shown in Fig. 3. This system consists of five dispatchable DG units including two micro-turbines (MT_1 & MT_2), two fuel cells (FC_1 & FC_2), and one gas engine (GE). Also, five RES plants including three WTs and two PVs are connected in different buses. The data associated with the installed generation units are given in Table 2, [20].

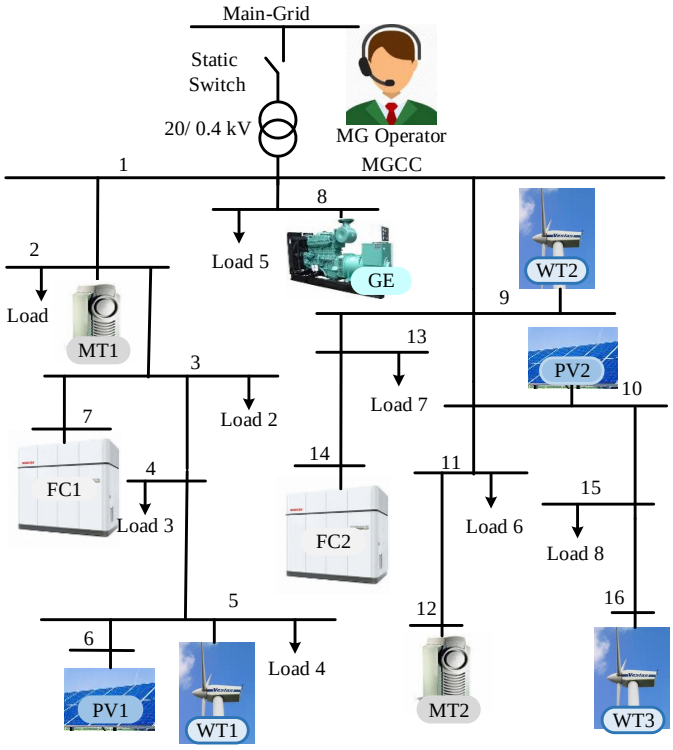

Fig. 3. Single line diagram of the simulated MG.

Also, the hourly forecasted active power outputs of WT and PV plants are depicted in Fig. 5 [20]. It is assumed that the PV plants operate at unity power factor while the WT units operate at 0.95 legging power factor. Moreover, the MG feeds eight similar three-phase balanced aggregated loads ($load_1$ to $load_8$ in Fig. 3) that are voltage and frequency dependent. Moreover, these loads and are equipped with EMC and could participate in DR program. It is assumed that the power factor of each load group is 0.95 lagging. The costs of demand-side reserves are 2 and 1.7 cent/kW for up and down spinning reserves, respectively. Besides, the generation costs of WT and PV systems are 10.63 and 54.84 cent/kWh, respectively, and the value of lost load (VOLL) is 1000 cent/kWh [20]. Moreover, it is assumed that the prices for buying and selling deviation power from unit *i*, WT and PV are equal to their energy bids in day-ahead market. Hourly load profile and energy price at TOU tariff of the study MG in a given day is also shown in Fig. 5. In this study, daily load of MG is divided into three different periods, namely valley period (00:00–5:00), off-peak periods (5:00–10:00, 16:00–19:00 and 22:00–24:00) and peak periods (11:00–15:00 and 20:00–22:00). Also, the price elasticity of the loads is adopted from [26]. It should be noted that the nominal value for the MG bus voltages is 400V, and the nominal system frequency is considered to be 60 Hz. Moreover, voltage magnitude at all buses and the system frequency can exceed up to ±5 % and ±1.5 % from their nominal values, respectively.

Table 2. Technical specifications of the simulated MG components.

DG	P^{min} (kW)	P^{max} (kW)	A (cents/kWh)	B (cents)	SUC (cents)	SDC (cents)	C^{R^U} (cents)	C^{R^D} (cents)	$C^{R^{NS}}$ (cents)	$m_{p,i}$	Emission (kg/kWh)
MT1	25	150	185.06	4.47	9	8	2.1	2.1	2.1	0.05	0.550
MT2	25	150	185.06	12.57	9	8	2.1	2.1	2.1	0.05	0.550
FC1	20	100	355.18	4.14	16	9	1.5	1.5	1.5	0.025	0.377
FC2	20	100	355.18	14.24	16	9	1.5	1.5	1.5	0.025	0.377
GE	35	150	312.00	7.42	12	8	1.7	1.7	1.7	0.01	0.890

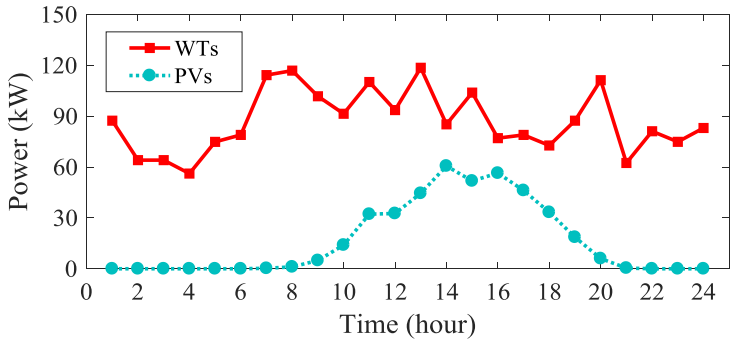

Fig. 4. The output power of WT and PV plants

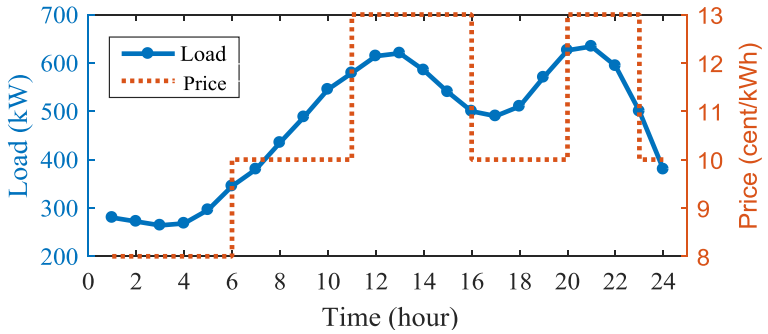

Fig. 5. Total load of MG and energy price at TOU tariff.

The proposed optimization modeling is examined over a 24-hour scheduling horizon. To simulate the environmental/behavioral uncertainties within the system, 2000 initial scenarios are generated based on PDFs to represent different values for wind and PV output power uncertainties as well as uncertainties in demand-side

participation. In the next step, by implementing an efficient scenario reduction algorithm, 25 scenarios are chosen that represent well enough the uncertainties. The reduced scenarios are then applied to the proposed MIP-based optimization model to maximize the expected profit of MG operator as well as to ensure system voltage and frequency security. The optimization is carried out by CPLEX solver using GAMS software [34] on a PC with 4 GB of RAM and Intel Core i7 @ 2.60 GHz processor.

We consider four cases for analyzing the effect of TOU-based DR program on voltage and frequency deviations. In case 0, the MGO maximizes his expected profit without DR participation under TOU program. In cases 1, 2 and 3 customers participate in DR programs and their level of contributions are considered as 20%, 40% and 60%, respectively. Fig. 6 shows the hourly load profiles of the MG in these four cases. As it can be observed, with the participation of customers in TOU program, the total demand decreases during peak hours when electricity prices have high values and increases during off-peak or valley periods when prices are relatively lower. Peak demand reductions from DR actions in cases 1, 2 and 3 are 3.6%, 7.6% and 11%, respectively.

The optimized values of the expected profit of MGO, customers' payment, cost of DG units, pollutant emissions and cost of EENS are given in Table 3. As seen in this table, with increasing customers' participation in TOU program, the expected MGO profit is increased. The reason is that the expensive units are not dispatched to satisfy the demand at peak hours as the peak load has been reduced through DR programs.

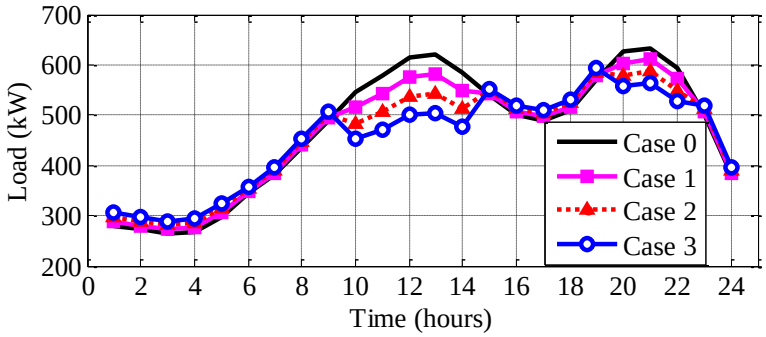

Fig. 6. Hourly load profile in different cases.

Table 3. The optimization values of the objective function in different cases.

Attribute	Case 0	Case 1	Case 2	Case 3
Expected profit of MG operator (cents Day^{-1})	29682.10	37726.67	39967.84	41409.29
Customers' payments as bills (cents Day^{-1})	124766.00	122625.04	120544.07	118433.11
Cost of DG units (cents Day^{-1})	78203.49	75824.37	74145.58	72842.36
Pollutant emissions (kg Day^{-1})	6486.85	6484.85	6441.48	6324.35
Cost of EENS (cents Day^{-1})	6093.79	345.43	238.56	212.04

Variations of system frequency under different working scenarios and different hours in a given day for different cases are shown in Fig. 7. It can be seen in all case studies that the system frequency is regulated well enough around the nominal value (i.e. 60 Hz) through optimal coordination of DERs and DR actions based on a meaningful trade-off between technical and economical issues. The highest frequency drop (worst case scenario) is related to scenario 21 where demand level and RESs generation have their maximum and minimum values, respectively. The other extreme case happens in scenario 5 where the load consumption and RESs generation have their minimum and maximum levels, respectively and the system frequency jumps to the highest value. It can be also observed that with active participation of end-users in DR programs (especially during 11:00 to 15:00 when the loads have higher demand elasticity), the system frequency goes under less variation as more reserve is allocated by responsive loads.

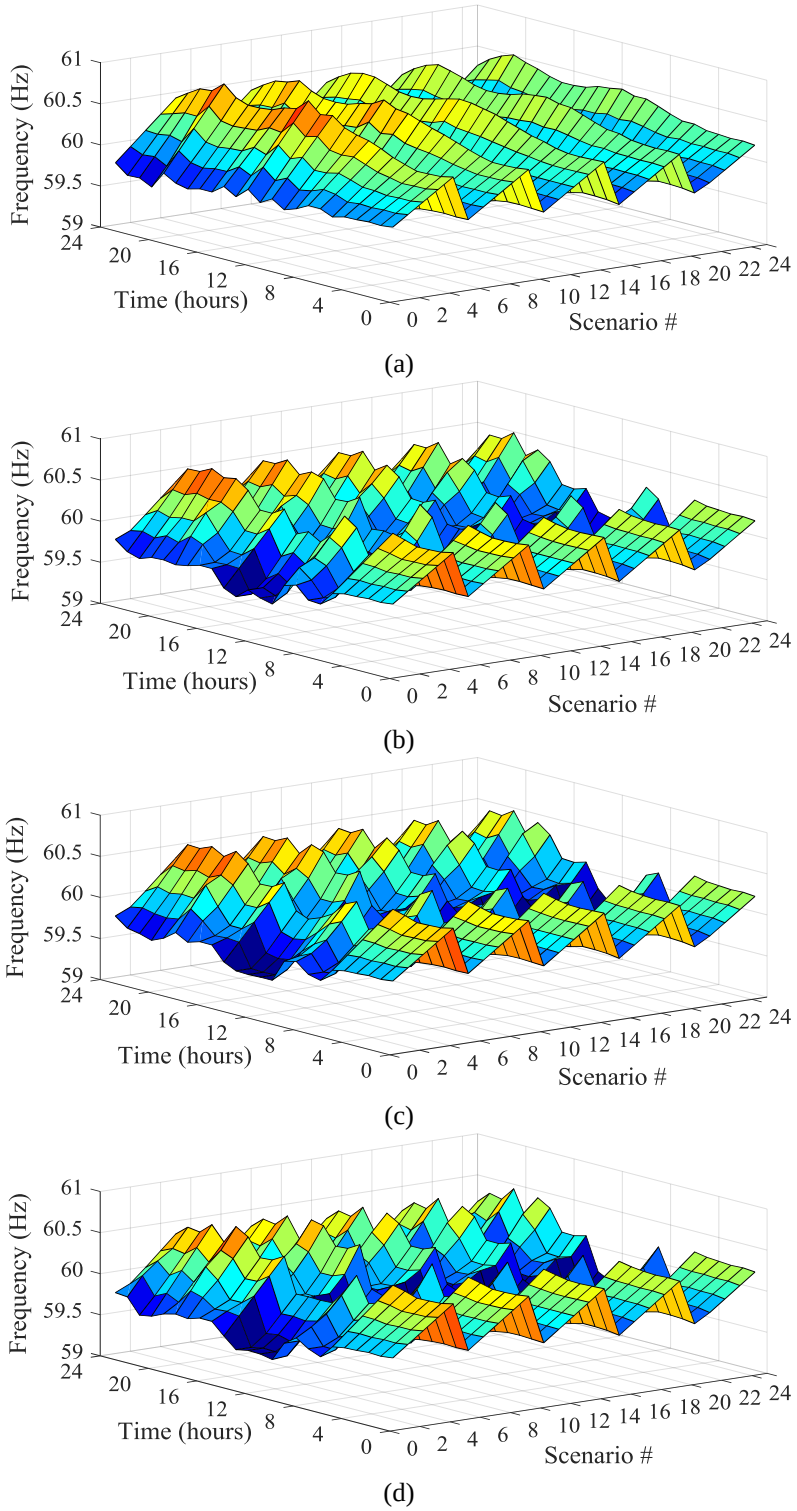

Fig. 7. Variation of MG frequency in different cases, (a) case 0, (b) case 1, (c) case 2, (d) case 3.

Average values of the system frequency in different cases and different hours are depicted in Fig. 8. As shown in this figure, the average values of frequency in all cases are the same during the valley period as in this time interval the total demand is very low and DG units could effectively support the load. Therefore, TOU-based DR program has not significantly affected on the average values of frequency at the valley period. But, at other hours of the day, especially

at hours 11:00 to 15:00, average of frequency has changed more with applying DR. Since, DR resources allocate more reserve capacity for frequency regulation at 11:00 to 15:00 based on the proposed optimal scheduling.

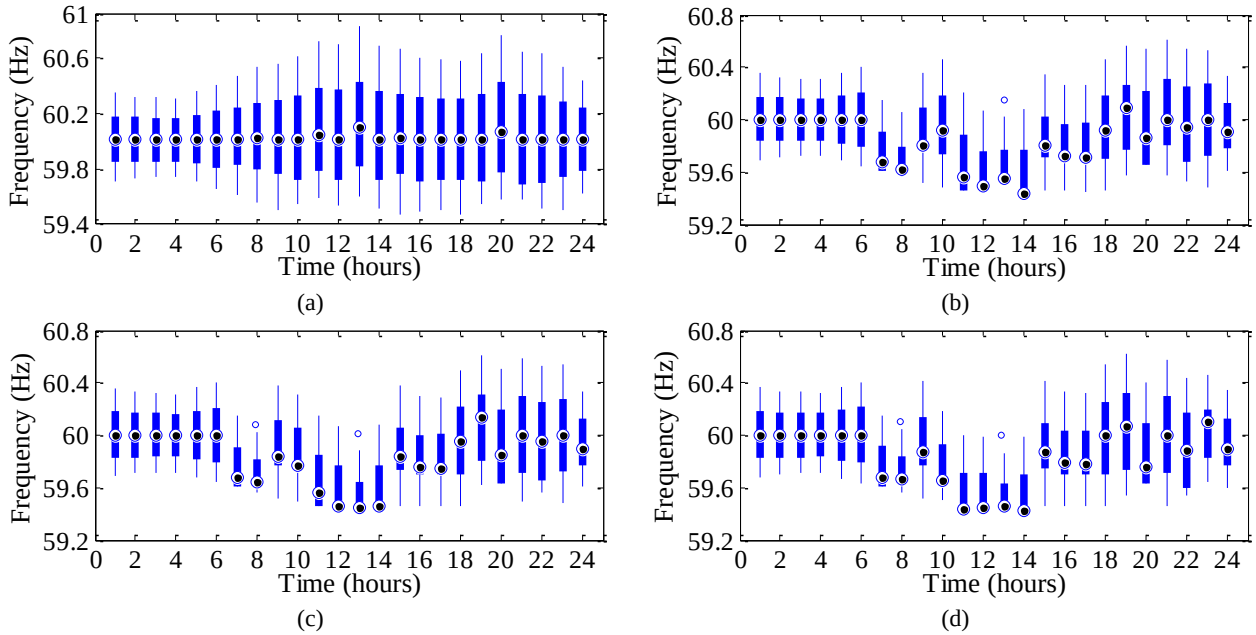

Fig. 8. Average of hourly static frequency in different cases, (a) case 0, (b) case 1, (c) case 2, (d) case 3.

The results obtained from the proposed approach for solving the stochastic security-constrained energy and reserve scheduling problem with considering TOU-based DR program are presented in Table 5 and compared with the results obtained from two other approaches in related literature. The numerical results show the performance of the proposed approach against existing methods in terms of computational time and voltage and frequency regulation capability (standard deviation (SD)) indices averaged over 25 working scenarios. As can be seen in this table, using the method presented in [17] and [19], in which DC-OPF is used, results in lower run times compared to other methods, however the voltage and frequency standard deviations (SD) are considerably high (less accuracy). Also, by using the method presented in [24] and [25], in which AC-OPF is used, although the voltage and frequency deviations can be relatively decreased, computational time is relatively high. On the other hand, the proposed method in this paper demonstrates a better performance in terms of voltage and frequency regulations. It also solves the optimization model in a reasonable time which is comparable with the existing methods. It should be noted that as the solution approaches differ in our comparative study, so do the computational burdens.

To validate the correctness of the presented results analytically, the generation level of DG units and their power set-point in different cases are studied in two scenarios. Here, scenarios 5 and 21 are chosen in which the frequency has the highest and the lowest values compared to other scenarios. The results for hours 13:00 and 21:00 for these scenarios are presented in Table 6. The optimal power set-points of DR and DG resources are adjusted by MGCC considering economic operation and security constraints. Based on the results listed in this table, the system frequency can be also calculated analytically. For example, in four cases in scenario 5 and at hour 13:00, the frequency equals to:

$$f_{case0} = 60 - \frac{(57.18+25+100+123.78)-(92.45+114.47+100+150)}{5+(\frac{1}{0.05})+(\frac{1}{0.05})+(\frac{1}{0.025})+(\frac{1}{0.01})} = 60.816Hz$$

$$f_{case1} = 60 - \frac{(94.3+53.12+93.26+150)-(94+80+93+150)}{5+(\frac{1}{0.05})+(\frac{1}{0.05})+(\frac{1}{0.025})+(\frac{1}{0.01})} = 60.150Hz$$

$$f_{case2} = 60 - \frac{(150+25+78.47+148.84)-(150+81.20+148.84)}{5+(\frac{1}{0.05})+(\frac{1}{0.05})+(\frac{1}{0.01})} = 60.015Hz$$

$$f_{case3} = 60 - \frac{(150 + 41.95 + 150) - (149.64 + 41.95 + 150)}{5 + (\frac{1}{0.05}) + (\frac{1}{0.05}) + (\frac{1}{0.01})} = 59.998 Hz$$

Table 5: Obtained results for stochastic scheduling problem on the MG test system by different solution approaches.

Solution Approaches	Case of study	Solution approaches	Run-time (sec)	SD of frequency (Hz)	SD of voltage (pu)
The model presented in reference [19]	Case 0	DC-OPF	613	0.133	0.123
	Case 1	DC-OPF	642	0.114	0.119
	Case 2	DC-OPF	646	0.111	0.111
	Case 3	DC-OPF	652	0.103	0.107
The model presented in reference [19]	Case 0	DC-OPF	634	0.121	0.112
	Case 1	DC-OPF	678	0.108	0.108
	Case 2	DC-OPF	687	0.105	0.106
	Case 3	DC-OPF	691	0.098	0.101
The model presented in reference [24]	Case 0	AC-OPF	1269	0.123	0.120
	Case 1	AC-OPF	1298	0.111	0.114
	Case 2	AC-OPF	1309	0.109	0.108
	Case 3	AC-OPF	1312	0.107	0.103
The model presented in reference [25]	Case 0	AC-OPF	1347	0.111	0.109
	Case 1	AC-OPF	1453	0.102	0.104
	Case 2	AC-OPF	1480	0.094	0.102
	Case 3	AC-OPF	1498	0.090	0.097
The proposed Model	Case 0	AC-OPF	1019	0.102	0.106
	Case 1	AC-OPF	1076	0.097	0.102
	Case 2	AC-OPF	1088	0.093	0.101
	Case 3	AC-OPF	1094	0.087	0.095

Table 6. Generation levels of DG units and their reference power set-point (kW) in scenario 5 and 21 during peak hours (13:00 and 21:00) in different cases.

Scenario #	Hour	DG	Case 0		Case 1		Case 2		Case 3	
			Generation level	Power set-point	Generation level	Power set-point	Generation level	Power set-point	Generation level	Power set-point
Scenario 5	13:00	MT_1	53.412	92.448	87.295	87.295	150	150	150	147.229
		MT_2	25	114.472	25	85.889	25	66.224	27.10	31.692
		FC_1	100	100	96.422	96.422	0	0	0	0
		FC_2	0	20	0	0	0	0	0	0
		GE	119.963	130	150	150	150	150	150	150
	21:00	MT_1	115.252	115.252	124.125	124.125	123.521	123.521	150	150
		MT_2	55.871	133.469	44.021	144.021	41.571	141.571	52.08	120.8
		FC_1	92.459	92.459	83.494	83.494	83.088	83.088	0	0
		FC_2	100	80	20	36.012	20	35.183	32.147	92.147
		GE	150	150	150	150	150	150	141.804	136.887
Scenario 21	13:00	MT_1	150	92.448	150	87.295	150	150	150	147.229
		MT_2	135.594	114.472	85.889	85.889	66.224	66.224	31.692	31.692
		FC_1	100	100	100	96.422	100	0	100	0
		FC_2	0	0	0	0	0	0	0	0
		GE	150	150	150	150	150	150	150	150
	21:00	MT_1	150	115.252	150	124.125	150	123.521	150	150
		MT_2	150	133.469	144.021	144.021	141.571	141.571	120.8	120.8
		FC_1	100	92.459	100	83.494	100	83.088	100	0
		FC_2	100	80	36.012	36.012	35.183	35.183	92.147	92.147
		GE	150	150	150	150	150	150	150	136.887

The frequency profiles regarding the aforementioned scenarios for all cases during the 24h scheduling time horizon are depicted in Fig. 9. The presented values in this figure are validated analytically (as done above) and the obtained results show the correctness of the results from presented approach. As it can be seen, in both scenarios the frequency is kept within the acceptable range. In scenario 5-case 0 (Fig. 9-(a)), the frequency deviation is at the maximum allowable limit (i.e., 1.5% more than its nominal value), however in other cases the frequency deviations have lower values and remain within more secure ranges, especially during peak hours, due to the participation of consumers in DR program. Moreover, as can be seen in Fig. 9-(b), the frequency deviation is increased in some hours (e.g., 1:00 to 5:00 and 9:00 to 18:00) with applying DR due to the trade-off between technical and economic issues.

Also, the proposed method can also guarantee the system frequency and nodal voltages to be kept within their secure range following a sudden outage of a generation unit, a change in the real/reactive power consumption or generation and so on. To evaluate the performance of the proposed method under different working conditions that are more likely to happen contingency analysis of the system is illustrated in Fig. 10 during the mentioned scenarios. Forced outage (loss) of a DG unit (e.g., unit 1) is simulated and the system frequency response after the event is captured. As it is observed, although a contingency is triggered (outage of a generating), the system frequency remains within its acceptable range through optimal coordination of distributed energy sources and responsive loads (N-1 criteria is met appropriately). It should be noted a reliable operating condition would also be observed in case of other generation units' outages or sudden loss of loads. However, we have just reported on one typical case as an illustrative example. Based on the numerical results, it is also observed that in different working conditions (normal or faulty), with the application of TOU program the frequency variation decreases and remains in a secure range. Nevertheless, by enabling DR programs and as the result with more participation of responsive loads, the reserve capacity of generation units would increase that yields to improving the frequency security margin.

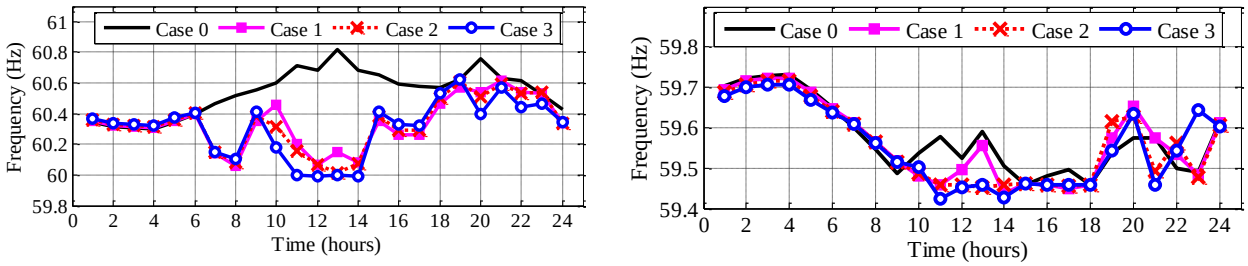

Fig. 9. Hourly frequency profile of different cases in (a) scenario 5 and (b) scenario 21.

Because, as it can be seen from, with consideration of DR influence on frequency regulation, the difference between DGs generation level and their power set-point is lower than that of in case 0, so, the frequency deviations are relatively higher in the cases with DR.

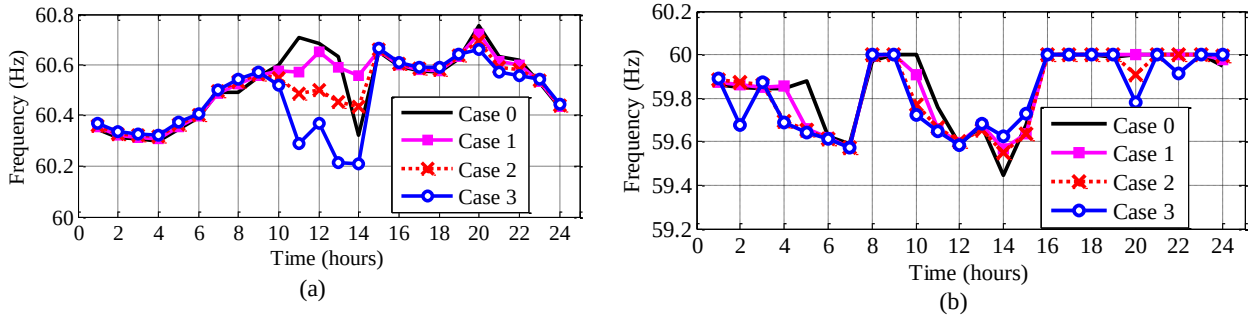

Fig. 10. Hourly frequency profile of different cases in (a) scenario 5 and (b) scenario 21.

Fig. 11 illustrates the nodal voltage fluctuations as well as the average bus voltages in different cases over the scheduling horizon. Since the reactive power level in a bus mainly determines the voltage magnitude, it can be expected that the voltage profile in a given bus can be affected by the implementation of DR actions. In a bus with a DG unit, if the amount of injected reactive power is reduced, then voltage magnitude will be decreased and in a load

bus, if the demand load is reduced, then the reactive power consumption will be decreased and the voltage will rise. However, it should be also noted that the reactive power injected or absorbed by a generating unit can change voltage magnitude of other buses. As it can be seen, the average voltage magnitude at some buses in case 0 is more than that of other cases. Since, higher numbers of DG units are committed in case 0, more reactive power injected to the system which in turn boosts the voltage at some points. With increasing DR contributions, however, the nodal voltages are affected differently. This implies that the average voltage in some buses with high DR support decreases due to reductions in the net reactive power injected into those buses while the opposite happens to the buses without or with lower DR support.

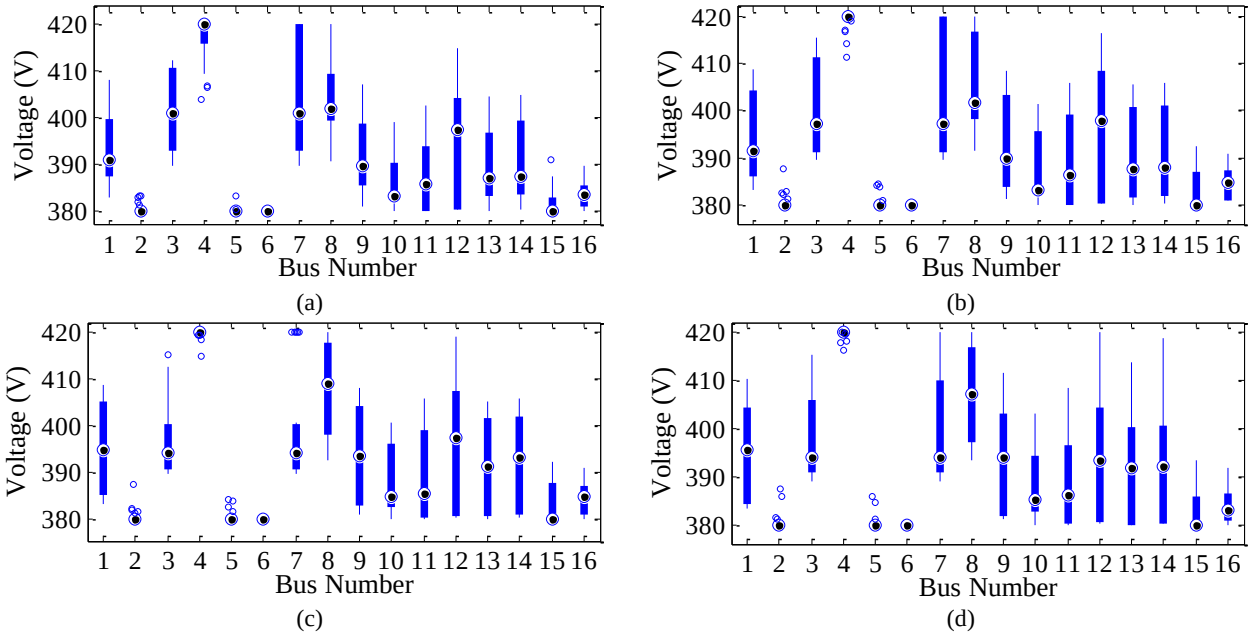

Fig. 11. Average of hourly voltage in different cases, (a) case 0, (b) case 1, (c) case 2, (d) case 3.

In order to investigate the system nodal voltages, the hourly voltage profile of four typical buses 1, 7, 12 and 16 are plotted in Fig. 12.

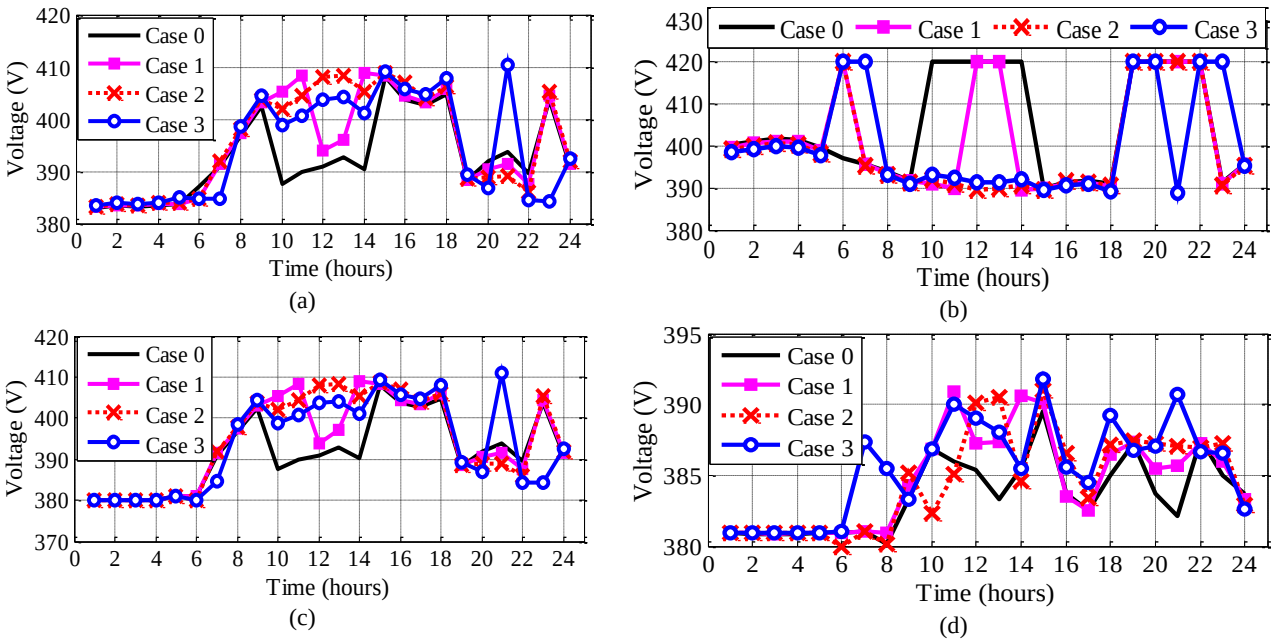

Fig. 12. Hourly voltage magnitude of different cases in (a) bus 1, (b) bus 7, (c) bus 12 and (d) bus 16.

As can be seen, with increasing DR participation in TOU-based program, the voltage magnitudes change at some hours. In the valley period (i.e., 1:00 to 5:00), the voltage magnitude is less sensitive to DR than in the peak period (such as 10:00 to 14:00). Since, in the peak period more load reduction is triggered and less expensive generating units are dispatched due to the lower load levels, less reactive power would be injected into buses and as the result greater voltage drops may be observed. On the other hand, at the low load intervals, especially during the valley period the voltage profile at all cases are somehow the same. This happens because of the aggregated load in these hours and in all four cases is almost similar which in turn necessitates similar unit commitment pattern and supplement of local reactive power accordingly. As a result with applying DR the voltage magnitude is significantly improved, especially in peak periods, but in other periods participation of responsive loads may reduce security margins.

IV. Conclusions

This paper presented a stochastic model for security-constrained energy and reserve scheduling of an islanded MG with considering TOU-based DR program. In this regard, a two-stage stochastic model was proposed for optimal coordination of DG units and responsive loads in order to maximize the expected MGO profit with considering voltage and frequency security constraints. To study the effect of uncertain parameters (such as wind and PV productions and also load consumption) on the proposed scheduling problem, a scenario-based stochastic programming method was employed. Moreover, an ACOPF approach was applied to observe the actual operating conditions and to determine the effect of customers' participation in TOU- DR program on MG voltage and frequency security. Simulation results demonstrated that the optimal coordination of DERs and DR actions, could not only meet the system's objectives, but also satisfy the system's technical/security constraints in an appropriate way. It was also observed that the customers' participation in energy and reserve scheduling, could have significant effects on the voltage and frequency response of the system in steady-state. Based on the numerical results, it was also observed that in different conditions (normal or faulty), by enabling TOU-DR programs and as the result with more participation of responsive loads, the reserve capacity of generation units would increase that yields to improving the frequency security margin. In other word, with higher demand-side participation in energy and reserve provision, larger capacity from DG units would be available which in turn assures better frequency regulation even during the peak load periods. Moreover, with increasing DR participants, the MG bus voltages change at some hours, especially at peak periods. At some buses with high DR support, the average nodal voltages could decrease due to reduction in the net reactive power injected into those buses while the opposite could happen to the buses without or with lower DR support. Also, with increasing DR participants, the number of committed units decreases and so does the reactive power injection which in turn reduces certain bus voltages. Based on the proposed method, operator could track the voltage and frequency profiles of MG at the operation conditions and ensure the system security.

Our future effort will be mainly focused on developing an optimal risk-constrained stochastic programming with considering price-based DR programs in order to properly control the MG expected voltage and frequency deviations in a cost-effective scheme. More investigations will be also conducted on real-world uncertainties of DR resources and their influence on energy and reserve scheduling.

References

[1] Marzband, M., Alavi, H., Ghazimirsaeid, S.S., Uppal, H., and Fernando, T., "Optimal energy management system based on stochastic approach for a home Microgrid with integrated responsive load demand and energy storage," Sustain. Cities Soc., 28, 256–264, (2017).

[2] Mokhtari G., Anvari-Moghaddam A., and Nourbakhsh G., "Distributed Control and Management of Renewable Electric Energy Resources for Future Grid Requirements," Energy Management of Distributed Generation Systems Dr. Eng. Lucian Mihet (Ed.), ISBN: 978-953-51-4708-4, InTech, (2016)

[3] Khodaei A., "Microgrid optimal scheduling with multi-period islanding constraints," IEEE Trans. Power Syst. 29(3), 1383-1392 (2014).

[4] Anvari-Moghaddam A., Monsef H., and Rahimi-Kian A., "Cost-Effective and Comfort-Aware Residential Energy Management under Different Pricing Schemes and Weather Conditions," Energy and Buildings 86:782-793 (2015).

[5] Lv K., Tang H., Li Y., and Li X., "A learning-based optimization of active power dispatch for a grid-connected microgrid with uncertain multi-type loads," Journal of Renewable and Sustainable Energy 9, 065901 (2017).

[6] Dehghani H., Faramarzi D., Vahidi B., and Saeidi M., "A probabilistic method for cost minimization in a day-ahead electricity market considering wind power uncertainties" Journal of Renewable and Sustainable Energy 9, 063301 (2017).

[7] Vahedipour-Dahraie, M., Rashidizaheh-Kermani, H., Najafi, H. R., Anvari-Moghaddam, A., and Guerrero, G. M., "Coordination of EVs participation for load frequency control in isolated microgrids," Appl. Sci. 7(6-539), 1-16,

(2017)
[8] Sattarpour T., Nazarpour D., and Golshannavaz S., "A multi-objective HEM strategy for smart home energy scheduling: A collaborative approach to support microgrid operation," Sustainable Cities and Society, 37, 26-33, (2018).
[9] Anvari-Moghaddam A., Vasquez J. C., Guerrero J. M., Monsef H., and RahimiKian A., "Efficient energy management for a grid-tied residential microgrid," IET Gener. Transm. Distrib., 11 (11), 2752-2761 (2017).
[10] Moradi M.H., Reisi A.R., and Hosseinian S.M., "An optimal collaborative congestion management in national grid based on implementing demand response," Journal of Renewable and Sustainable Energy 9, 025502 (2017).
[11] Gholami A., Shekari T., Aminifar F., and Shahidehpour M., "Microgrid Scheduling with Uncertainty: The Quest for Resilience," IEEE Trans. Smart grid, 30(3), 1337-1350 (2016).
[12] Moshari A., Ebrahimi A., and Fotuhi-Firuzabad M., "Short-Term Impacts of DR Programs on Reliability of Wind Integrated Power Systems Considering Demand-Side Uncertainties," IEEE Trans. Power Syst., 31(3), 2481-2490 (2016).
[13] Vahedipour-Dahraie M., Najafi H.R., Anvari-Moghaddam A., Guerrero J.M., "Study of the Effect of Time-Based Rate Demand Response Programs on Stochastic Day-Ahead Energy and Reserve Scheduling in Islanded Residential Microgrids," Appl. Sci.,7 (4-378),1-19 (2017).
[14] Nan S., Zhou M., Li G., "Optimal residential community demand response scheduling in smart grid," Applied Energy, 210, 1280-1289, (2018).
[15] Conteh F., Tobaru S., Howlader R., Yona A., and Senjyua T., "Energy management systems for hybrid distributed generation sources in grid connected and stand-alone micro-grids," Journal of Renewable and Sustainable Energy 9, 065301 (2017)
[16] Di Somma M., Graditi G., Heydarian-Forushani E., Shafie-khah M., Siano P., "Stochastic optimal scheduling of distributed energy resources with renewables considering economic and environmental aspects," Renewable Energy, 116, pp. 272-287, (2018).
[17] Aghajani G.R., Shayanfar H.A. Shayeghi H., "Demand side management in a smart micro-grid in the presence of renewable generation and demand response," Energy, 126, 622-637 (2017).
[18] Nikmehr N., Najafi-Ravadanegh S., Khodaei A., Probabilistic optimal scheduling of networked microgrids considering time-based demand response programs under uncertainty, Applied Energy, 198, 267-279 (2017).
[19] Aghaei J., Ahmadi A., Rabiee A., Agelidis V. G., "Muttaqi K. M., and Shayanfar H., Uncertainty management in multiobjective hydro-thermal self-scheduling under emission considerations," Appl Soft Comput, 37, 737-750 (2015).
[20] Rezaei N., and Kalantar M., "Stochastic frequency-security constrained energy and reserve management of an inverter interfaced islanded microgrid considering demand response programs," Int. J. Electr. Power Energy Syst., 69, 273-286 (2015).
[21] Rezaei N., and Kalantar M., "Economic–environmental hierarchical frequency management of a droop-controlled islanded microgrid," Energy Convers Manage, 88, 498-515 (2014).
[22] Rezaei N., and Kalantar M., "Smart microgrid hierarchical frequency control ancillary service provision based on virtual inertia concept: An integrated demand response and droop controlled distributed generation framework," Energy Conversion and Management, 92, 287-301 (2015).
[23] Bayat M., Sheshyekani K., and Rezazadeh A., "A unified framework for participation of responsive end-user devices in voltage and frequency control of the smart grid," IEEE Trans. Power Syst., 30(3), 1369-1379 (2015).
[24] Bayat M., Sheshyekani K., Hamzeh M., and Rezazadeh A., "Coordination of Distributed Energy Resources and Demand Response for Voltage and Frequency Support of MV Microgrids," IEEE Trans. Power Syst., 31(2), 1506-1516 (2016).
[25] Rezaei N., and Kalantar K., A novel hierarchical energy management of a renewable microgrid considering static and dynamic frequency Journal of Renewable and Sustainable Energy 7, 033118 (2015).
[26] Vahedipour-Dahraie M., Rashidizadeh-Kermani H., Najafi H. R., Anvari-Moghaddam A., and Guerrero, J. M. "Stochastic Security and Risk-Constrained Scheduling for an Autonomous Microgrid with Demand Response and Renewable Energy Resources," IET Renewable Power Generation, 11(14), 1812-1821 (2017).
[27] Alemany J., and Magnago F., "Benders decomposition applied to security constrained unit commitment: Initialization of the algorithm," International Journal of Electrical Power & Energy Systems, 66, 53-66 (2015).
[28] Rabiee A., and Soroudi A., "Stochastic multi-period OPF model of power systems with HVDC-connected intermittent wind power generation," IEEE Trans. Power Del., 29(1), 336-344 (2014).
[29] Koudouris G., Dimitriadis P., Iliopoulou T., Mamassis N., and Koutsoyiannis D., "Investigation on the stochastic nature of the solar radiation process," Energy Procedia, 125, 398-404 (2017).
[30] Arthur D., and Vassilvitskii S., "K-means++: The advantages of careful seeding," In Proc. 18th Annu. ACM-

SIAM Symp. Discrete Algorithms (SODA ‘07), New Orleans, LA, USA, 1027-1035 (2007).
[31] Löhndorf N., “An empirical analysis of scenario generation methods for stochastic optimization,” European Journal of Operational Research, 255(1), 121-132 (2016).
[32] Anvari-Moghaddam A., Shafiee Q., Vasquez J. C., and Guerrero J. M., “Optimal Adaptive Droop Control for Effective Load Sharing in AC Microgrids,” 42nd Annual Conf. IEEE Ind. Electron. Society (IECON’16), October 24-27, Florence, Italy, (2016).
[33] Hazra J., and Sinha A. K., “Congestion management using multi-objective particle swarm optimization,” IEEE Trans. Power Syst., 22(4), 1726-1734, (2007).
[34] Oua M., Xue Y., and Zhang X.P., “Iterative DC optimal power flow considering transmission network loss,” Electr Power Compon. Syst., 44(9), 955-965, (2016).
[35] Akbari T., and Tavakoli Bina M., “Linear approximated formulation of AC optimal power flow using binary discretisation,” IET Gener. Transm. Distrib., 10, 1117-1123, (2016).
[36] “The General Algebraic Modeling System (GAMS) Software,” online available at: https://www.gams.com.